Effect of Noncovalent Interactions on the *n*-Butylbenzene···Ar Cluster Studied by Mass Analyzed Threshold Ionization Spectroscopy and *ab initio* Computations

Xin Tong,[†] Jiří Černý,[†] and Klaus Müller-Dethlefs*[,†,‡]

The Photon Science Institute, Alan Turing Building, the School of Chemistry, and the School of Physics and Astronomy, The University of Manchester, Manchester M13 9PL, U.K.

Received: November 19, 2007; Revised Manuscript Received: April 5, 2008

Clusters of Ar bound to isomers of the aromatic hydrocarbon *n*-butylbenzene (BB) have been studied using two-color REMPI (resonance enhanced multiphoton ionization) and MATI (mass analyzed threshold ionization) spectroscopy to explore noncovalent vdW interactions between these two moieties. Blue shifts of excitation energy were observed for *gauche*-BB···Ar clusters, and red shifts for *anti*-BB···Ar clusters were observed. Adiabatic ionization energies (IEs) of the conformer BB-I···Ar and BB-V···Ar were determined as 70052 and 69845 ± 5 cm^{-1}, respectively. Spectral features and vibrational modes were interpreted with the aid of UMP2/cc-pVDZ *ab initio* calculations. Data of complexation shifts of the alkyl-benzenes and their argon clusters were collected and discussed. Using the CCSD(T) method at complete basis set (CBS) level, interaction energies for the neutral ground states of BB-I···Ar and BB-V···Ar were obtained as 650 and 558 cm^{-1}, respectively. Combining the CBS calculation results and the REMPI and MATI spectra allowed further the determination of the interaction energies and the energetics of BB···Ar in the excited neutral S_1 and the D_0 cationic ground states.

1. Introduction

Covalent chemical bonds are generally well-understood and described by molecular *ab initio* computational methods. However, many molecular phenomena are determined by much weaker intermolecular forces that originate from noncovalent interactions and are of quite different nature. Bulk properties of gases, liquids, solutions and solids, as well as most biological processes are determined by noncovalent interactions.[1–6] Large van der Waals (vdW) complexes, consisting of an organic aromatic molecule bound to rare-gas atoms, are expected to provide basic information on the structural, energetic, and dynamic manifestations of intermolecular interactions in these well-characterized, large chemical systems.[7,8] With the increasing improvements in spectroscopic techniques, detailed studies of structure, energetics, and electronic-vibrational level structure along with the *intra-* and *inter*molecular dynamics can now be explored using clusters produced in molecular beams.[9–13]

In previous papers, we have explored noncovalent interactions within the *n*-butylbenzene monomer (BB).[14–16] Although the interactions between the alkyl side chain and the aromatic ring are not the determinant factor of the structure, it has been revealed that they play a very important role on the energetics in both the neutral S_0 and S_1 states and the cationic D_0 ground states. In this paper, a REMPI and MATI spectroscopic study of the vdW bound *n*-butylbenzene···argon (BB···Ar) cluster is presented in detail. This complex provides an opportunity to investigate the influence of an argon atom on the conformational preferences of the flexible BB molecule, which presents the noncovalent interaction in this molecular cluster. In addition, because many other examples of ZEKE/MATI studies for aromatic vdW complexes have been published,[13,17–21] the IE shifts of the alkylbenzene···Ar and benzene···Ar clusters are compared. The vdW bond strength is mainly determined by dispersion forces and the permanent multipole moments of the polarizabilities of the moieties, and typical bond energies (BE) vary from 5 to 200 meV, compared to 0.1 to 1 eV for hydrogen bonds.[22]

A large number of theoretical works has been dealing with rare gas clusters, including rare gas dimers and aromatic rare-gas clusters, and the best potential energy surfaces have been yet obtained by adjusting one or two parameters to fit experimental data. The only exception is the helium dimer, where an *ab initio* potential is even used for calibration.[23,24] The improvement of *ab initio* calculations can be basically targeted in two directions: use of (i) more sophisticated approximations of the *N*-electron wave function, i.e., inclusion of larger portions of correlation energy, and (ii) larger one-electron basis-sets.[25] For the description of van der Waals complexes, the coupled-cluster method covering single- and double-excitations iteratively and triple excitations perturbatively [CCSD(T) method] seems to recover the correlation energy satisfactorily and further corrections from higher excitations seem to be negligible. This was demonstrated[26] for the helium and neon dimer by performing CCSD(T), CCSDT and full CI calculations.

2. Experimental Setup

The experimental apparatus and setup are essentially the same as our study on BB monomer which was described in the previous paper.[16] However, there are two major differences for producing the BB···Ar cluster in the molecular beam. First, instead of using an 0.8 mm diameter General Valve nozzle, a smaller 0.5 mm one is used to increase the collision rate of the two moieties. Second, argon is used as a backing gas at a higher stagnation pressure of 4−6 bar to generate a sufficient yield of the clusters. On the basis of our earlier BB monomer and cluster spectra we estimated the rotational temperature around 2 K because we kept the jet expansion at the same conditions.[14,27]

* Corresponding author. E-mail: dethlefs@manchester.ac.uk.
† The Photon Science Institute and the School of Chemistry.
‡ School of Physics and Astronomy.

10.1021/jp710998m CCC: $40.75
Published on Web 06/06/2008

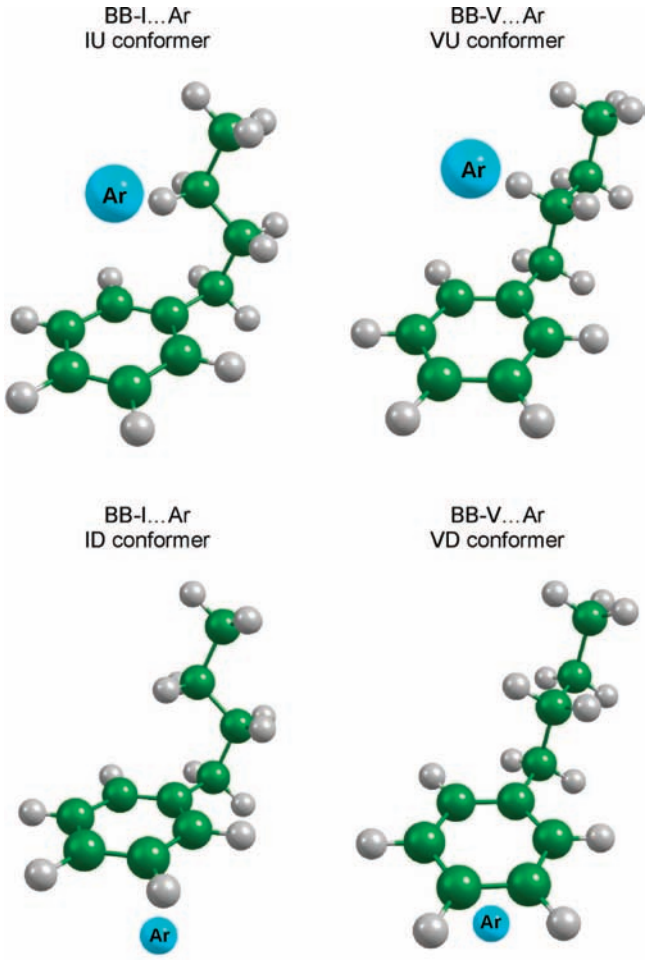

Figure 1. Geometric structures of the S_0 state of BB···Ar clusters calculated at the MP2/cc-pVTZ(BB)/aug-cc-pVTZ(Ar) level, with Ar atom labels.

The molecular beam interacts with the counter propagating, frequency-doubled outputs of two Nd:YAG pumped dye lasers (Radiant Narrowscan, Coumarin 153 and Sulfurhodamine B). Two-color (1 + 1′) REMPI spectroscopy was used to obtain the S_1 state spectrum, with the second photon's energy controlled to minimize spectral contamination *via* fragmentation of higher mass species. The pulse sequences, timings and field strengths used to obtain the REMPI spectra are identical to those in ref 28. For cationic states we use MATI spectroscopy to obtain the threshold ionization spectra of BB···Ar, because of the advantage of unambiguous mass-selectivity and equivalent resolution to ZEKE spectroscopy. The pulse sequences, timings and field strengths used to obtain the MATI spectra are identical to those in ref 29. Laser wavelengths were calibrated in vacuum wavenumbers by simultaneously recording iodine spectra.[30] Ionization energies are field corrected using $\Delta E\ (\mathrm{cm}^{-1}) = 4[F\ (\mathrm{V/cm})]^{1/2}$, where F presents the field strength.[31]

3. Computational Detail and Results

3.1. Structure. Figure 1 shows the structure of the BB···Ar clusters in the neutral ground states that were obtained using Gaussian 03, version C.02.[32] Both BB monomer I and V have two principle vdW ligand sites.[14] Here, we add "U" for labeling the ones having the Ar atom attached to the same side as the alkyl chain and "D" for the opposite side. The IU and VU conformers are expected of having lower total energies and higher stabilization energies due to the extra interaction between the Ar atom and the alkyl side chain, which is confirmed by the later calculations of stabilization energy in section 3.2. BB moieties in all the BB···Ar geometries show very little difference from respective BB monomers published in the previous paper.[14] Both IU and ID clusters have nonsymmetrical C_1 structures whereas BB-V···Ar clusters, VU and VD, keep the same C_s symmetry as BB-V monomer. For the BB moiety the cc-pVTZ basis set is used, whereas the augmented basis set (aug-cc-pVTZ) is used for the Ar atom. This is because it is important to include augmented functions in the basis set for the rare-gas atom Ar to fully recover the dispersion contribution to the noncovalent interaction. The reason for using the nonaugmented basis set, cc-pVTZ, for the BB monomer is not only to restrain the heavy cost of computation but also to avoid the overestimation of correlation energy within the BB moiety at the MP2 level of theory, resulting in poorer BB moiety geometries.[33] In addition, frequency calculations for the same basis sets were performed to ensure that optimized structures were local minima.

In the cationic state, due to high cost of computation and problems with spin contamination,[33] only the more stable clusters from each BB monomer, the IU and VU clusters, were optimized at the basis set level of cc-pVDZ for the BB moiety and the aug-cc-pVDZ for the Ar atom. In fact, the UMP2 calculation of BB-V···Ar gives one imaginary mode related to the aromatic ring stretch, which is likely to be caused by spin contamination. However, using restricted open shell method ROMP2, geometry and frequencies are confirmed and there is no imaginary vibration mode. Although one may argue about the efficiency of such basis sets for geometry optimization, this allows us to obtain reasonable harmonic frequencies (unscaled) for comparison with our MATI spectroscopy results which are discussed in section 4.2 and 4.3 at affordable low computational cost.

3.2. Complete Basis Set Limit of the Stabilization Energies. To correct the computed results for basis set incompleteness error at the MP2 level of theory, we employed the same two points Helgaker extrapolation schemes used for the previous BB monomer calculation.[16,34] For these single point energy calculations we utilized systematically augmented Dunning's basis sets (from aDZ to aQZ) rather than nonaugmented ones to reduce the extrapolation error. BSSE counterpoise correction and frozen-core approximation were applied throughout this study. Table 1 lists the results of stabilization energies of the BB···Ar cluster at the different basis sets and for extrapolation using the MP2 method. With the increase of the size of the basis sets, the stabilization energies increase for all the conformers. The IU conformer shows the highest stabilization energies at all levels with the Ar atom located on the same side as the alkyl chain. VU is a more stable conformer than the VD configuration. It is noticeable that the calculation shows that stabilization energies are not very different between the ID and VD conformers. This is because in both conformations, for which Ar atom and the alkyl side chain are on opposite sides of the aromatic ring, the alkyl side chain has very little influence on the vdW interaction between Ar atom and aromatic ring. The differences between aDZ→aTZ and aTZ→aQZ extrapolations are rather small compared to the differences between the nonextrapolated MP2 calculations. The aDZ→aTZ extrapolations ($-847\ \mathrm{cm}^{-1}$ for IU conformer and $-739\ \mathrm{cm}^{-1}$ for VU conformer) are closer to the CBS limit than aQZ calculation ($-822\ \mathrm{cm}^{-1}$ for IU conformer and $-718\ \mathrm{cm}^{-1}$ for VU conformer); therefore we can conclude that in such benzene derivates, one should expect two points aDZ→aTZ extrapolation

TABLE 1: Neutral Ground States Interactions Energy Calculation Results of the BB···Ar Clusters of Conformer I and V of BB Using the MP2 and Extrapolation Method (Values in cm^{-1})

	BB-I···Ar		BB-V···Ar	
	IU conformer	ID conformer	VU conformer	VD conformer
MP2/aDZ	−598	−441	−523	−442
MP2/aTZ	−773	−569	−674	−573
MP2/aQZ	−822	−608	−718	−611
MP2/aDZ→aTZ	−847	−624	−739	−628
MP2/aTZ→aQZ	−859	−637	−751	−640
$(\Delta E^{CCSD(T)} - \Delta E^{MP2})$/aDZ	208	181	192	183
CCSD(T)/aDZ→aTZ	−639	−443	−546	−446
CCSD(T)/aTZ→aQZ	−650	−456	−558	−457

gives the similar accuracy as a nonextrapolated aQZ calculation, which is much more computationally costly.

As stated in the Introduction, for the energy calculation of the van dear Waals complexes, the coupled-cluster method CCSD(T) is necessary. It has been found that the difference between CCSD(T) and MP2 interaction energies ($\Delta E^{CCSD(T)} - \Delta E^{MP2}$) exhibits only a small basis set dependence.[35,36] The complete basis sets (CBS) CCSD(T) interaction energy can hence be approximated as

$$\Delta E_{CBS}^{CCSD(T)} = \Delta E_{CBS}^{MP2} + (\Delta E^{CCSD(T)} - \Delta E^{MP2})_{\text{small basis set}} \quad (1)$$

In the present paper we use the reasonably small Dunning's basis set aug-cc-pVDZ basis set to evaluate the ($\Delta E^{CCSD(T)} - \Delta E^{MP2}$) correction term. These CCSD(T) calculations were carried out by the Molpro 2002 suite of programs.[37] On the basis of our previous work in phenol···Ar and phenol···Ar$_2$ we believe that the interaction energy of the complex is determined with the very high accuracy of better than about 10 cm^{-1}.[33,38] Table 1 also lists the coupled-cluster method corrected results. It is well-known that MP2 overestimates the dispersion forces, which leads to an overestimation of the interaction energy. Our ($\Delta E^{CCSD(T)} - \Delta E^{MP2}$) calculation results confirm this fact by giving the positive sign value round 200 cm^{-1} for all four clusters and it results in the reduced interaction energies for the CCSD(T)/CBS compared to the MP2/CBS calculations. However, the CCSD(T)/CBS results do not change the stabilization energy orders among the four BB···Ar clusters compared to the MP2/CBS calculations, keeping the IU and VU the favorite cluster configuration for BB-I···Ar and BB-V···Ar. A similar system, 2-phenylethanoll···Ar cluster, was studied by Neusser and co-workers, where high-resolution UV spectroscopy ad *ab initio* study at MP2/6-31G** level of theory were employed. Their findings also confirm that the Ar atom is located at the same side as the $-CH_2CH_2OH$ chain.[39]

4. Spectroscopic Study of n-Butylbenzene···Ar

4.1. REMPI Spectrum of *n*-Butylbenzene···Ar. The (1 + 1′) two-color REMPI spectrum of BB···Ar, recorded with the ionization laser set to 32700 cm^{-1}, is displayed in Figure 2b, and Figure 2a displays the corresponding spectrum of the BB monomers.[14]

The cluster REMPI spectrum is similar to the one for the monomer which can be divided into *gauche*- and *anti*-ranges. Four cluster origin bands were identified at 37522, 37519, 37553 and 37555 ± 0.5 cm^{-1}. Considering the intensity of the signal and relatively small shift in previous studies of vdW clusters, we propose to assign these four peaks to BB-III···Ar, BB-I···Ar, BB-IV···Ar and BB-V···Ar, respectively. Assignment of BB-I···Ar and BB-V···Ar has been confirmed by the MATI spectrum in the following sections 4.2 and 4.3. This assignment is supported by the relative intensities of the monomer and cluster isomer in the REMPI spectra. A few weak peaks are also observed in this REMPI spectrum; it is very difficult to assign them without further experimental work (e.g., hole-burning REMPI).[29] Table 2 lists the four BB···Ar excitation energies and their shift with respect to the monomers.

The most intriguing information obtained from the REMPI spectrum is that the two different types of BB conformers, *gauche*- and *anti*-, give different shift directions for the $S_1 \leftarrow S_0$ excitation energies. The phenomenon has been observed for

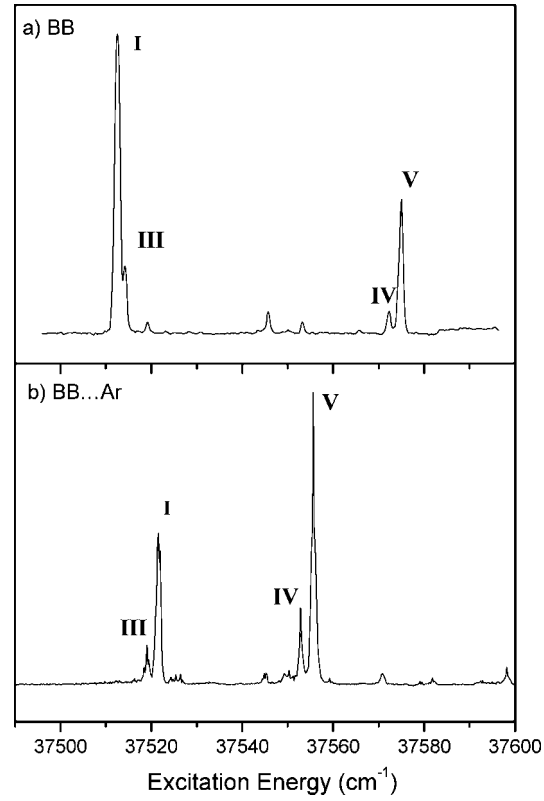

Figure 2. Two-color (1 + 1′) $S_1 \leftarrow S_0$ REMPI spectrum of (a) BB and (b) BB···Ar, recorded with the ionization laser set to 32700 cm^{-1}. Assignments of conformers I, III, IV and V of BB···Ar are included in (b).

TABLE 2: The $S_1 \leftarrow S_0$ Excitation Energies (in cm^{-1}) of Four Identified BB···Ar Clusters in the REMPI Spectrum (Figure 2), and the Shift Relative to the Respective Monomers

	conformer I	conformer III	conformer IV	conformer V
BB monomer	37513	37514	37572	37575
BB···Ar cluster	37522	37519	37553	37555
shift	8 (blue)	5 (blue)	−19 (red)	−20 (red)

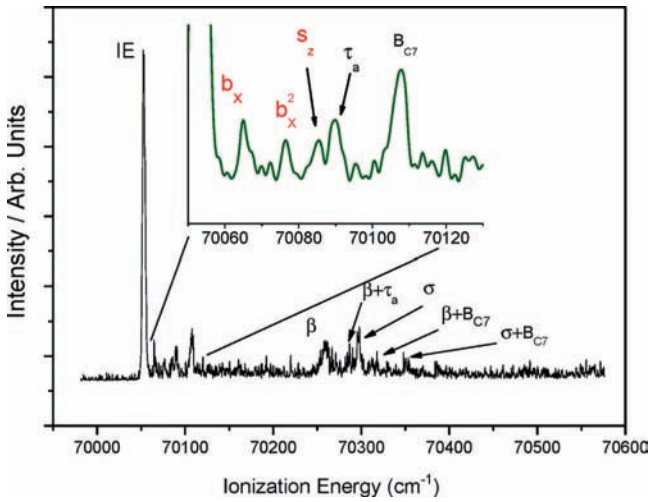

Figure 3. Two-color (1 + 1′) MATI spectrum of BB-I···Ar recorded *via* the $S_1 0^0$ intermediate state. Assignment of the intermolecular vibrational modes b_X and s_Z along with the intramolecular bending mode β, torsion mode τ_a, σ stretch mode and B_{C7} bending mode and their combinations are included on the spectrum.

TABLE 3: Frequencies (in cm^{-1}) and Assignments of the Vibrational Bands Observed in the MATI Spectrum of BB-I···Ar, compared with the Related Features in the BB-I Monomer

peak position	ion internal energy	intensity[a]	assignment	UMP2[b]	ion internal energy of BB monomer
70052	0	s	IE		
70065	13	w	b_X	13	
70076	24	vw	b_X^2		
			b_Y	33	
70085	33	vw	s_Z	48	
70090	38	w	τ_a	55	38
70107	55	m	B_{C7}	68	55
70259	207	m	β	208	197
70286	231	m	$\beta + \tau_a$		236
70297	245	m	σ	254	238
70313	261	vw	$\beta + B_{C7}$		254
70348	296	vw	$\sigma + B_{C7}$		

[a] Intensities are denoted as *s* = strong, *m* = medium, *w* = weak and vw = very weak. [b] Unscaled, using cc-pVDZ basis sets on BB moiety and aug-cc-pVDZ for Ar atom.

the first time in the 1:1 aromatic-rare-gas clusters studied here, and the most probable explanation is that the enhanced attractive interaction between the alkyl chain and aromatic ring in the *gauche*-conformer in the S_1 state has been weakened by the presence of the argon atom. In addition, it also indicates that the argon is attached to the same side of the aromatic ring toward which the alkyl chain bends.

4.2. MATI Spectrum of *n*-Butylbenzene-I···Ar. Figure 3 displays the MATI spectrum of BB-I···Ar clusters obtained *via* the $S_1 0°$ vibrationless origin. The prominent feature at 70052 ± 5 cm^{-1} is assigned as the IE because no additional spectral features were observed in the lower energy spectral range.

As stated in section 3.1, harmonic vibrational frequencies were determined to aid the assignment of the MATI spectra. In the low internal energy range of the MATI spectrum of BB-I···Ar clusters, three peaks relating to the intermolecular vibrational modes are observed. The b_X intermolecular bending mode and its overtone, b_X^2, are located at 13 and 24 cm^{-1}, respectively. The mode is well in line with our UMP2 calculated b_X frequency, which is at 13 cm^{-1}. The stretch between the BB

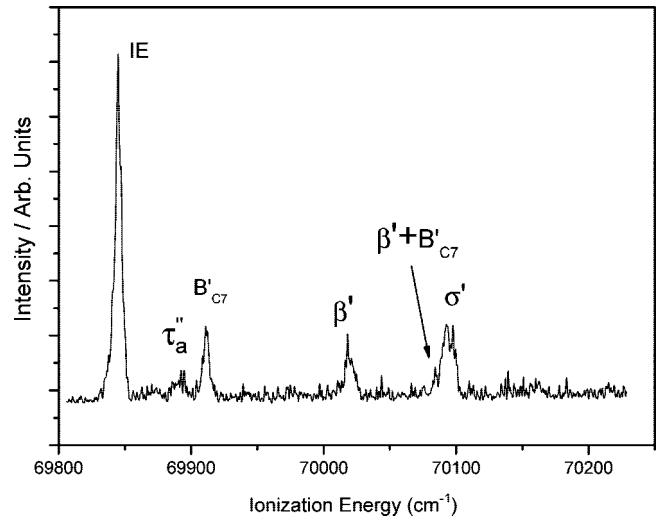

Figure 4. Two-color (1 + 1′) MATI spectrum of BB-V···Ar recorded *via* the $S_1 0^0$ intermediate state. Assignment of the intramolecular bending mode β, the torsion mode τ_a, the σ stretch mode, the B_{C7} bending mode and their combinations are included on the spectrum.

TABLE 4: Frequencies (in cm^{-1}) and Assignments of the Vibrational Bands Observed in the MATI Spectrum of BB-V···Ar, Compared with the Related Features in the BB-V Monomer

peak position	ion internal energy	intensity[a]	assignment	UMP2[b]	ion internal energy of monomer
69845	0	s	IE		
			b_X	23	
			b_Y	30	
			s_Z	52	
69892	47	w	τ_a''	53	43
69911	66	m	B_{C7}'	71	69
70018	173	m	β'	187	174
70043	198	vw	$B_{C7}'^3$		194
70084	239	w	$B_{C7}' + \beta'$		242
70093	248	s	σ'	256	248

[a] Intensities are denoted as s = strong, m = medium, w = weak and vw = very weak. [b] Unscaled, using cc-pVDZ basis sets on BB moiety and aug-cc-pVDZ for Ar atom.

TABLE 5: Summary of Stabilization, Excitation and Ionization Energy of BB···Ar Clusters (Values in cm^{-1})

	stabilization energy			excitation energy	ionization energy
	S_0	S_1	D_0	$S_1 \leftarrow S_0$	$D_0 \leftarrow S_0$
BB-I···Ar	650	641	746	37522	70052
BB-V···Ar	558	578	668	37555	69845

moiety and argon atom, s_z, appears at 33 cm^{-1} and our harmonic frequency calculation predicted the value of 48 cm^{-1}.

In the higher energy range, a series of intramolecular vibrational modes can also be assigned by comparison with the modes in the BB-I monomer MATI spectrum.[14] The peaks at 38 and 55 cm^{-1} are assigned to the alkyl side chain torsion mode, τ_a, and the scissor bend, B_{c7}, respectively; these modes have exactly the same frequency as in the BB-I monomer. The side chain bending mode, β, at 207 cm^{-1} and its combinations with the torsion mode τ_a at 231 cm^{-1}, and with B_{c7} at 261 cm^{-1} are also close to the related feature in the BB monomer (197, 236 and 254 cm^{-1}). The peak at 245 cm^{-1} is assigned to the stretching mode, σ, according to its appearance at 238 cm^{-1} in the BB-I monomer MATI spectrum. Finally, the combination mode of σ and B_{c7} appearing at 296 cm^{-1} was not observed in

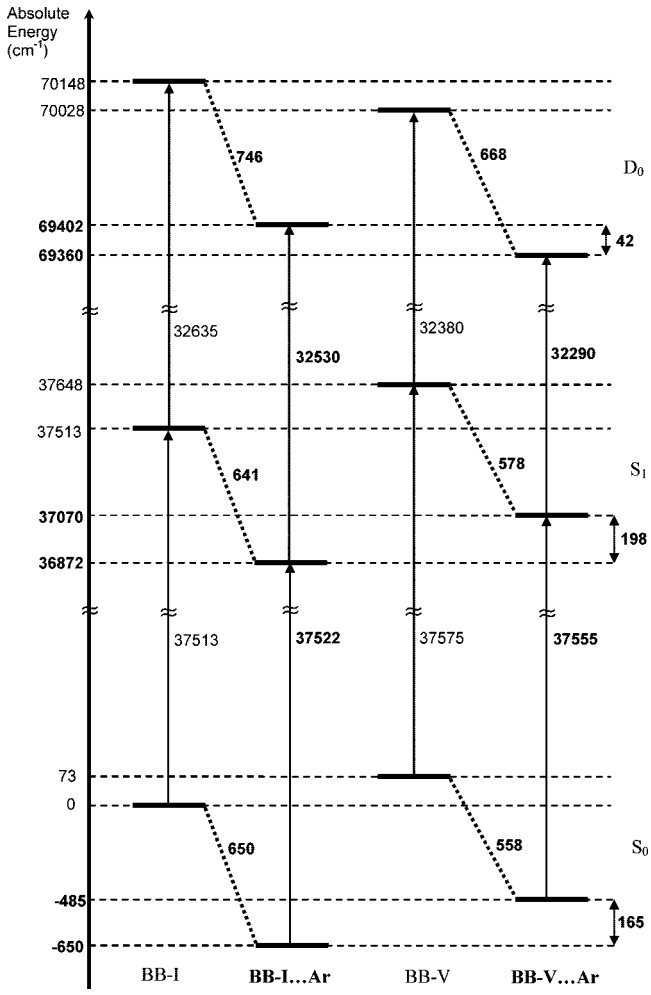

Figure 5. Schematic energy level diagram of BB-I···Ar, BB-V···Ar and their corresponding monomer illustrating the relative conformer energies in the S_0, S_1 and D_0 states. The values are in cm^{-1}.

the BB-I monomer MATI spectrum. All of the features observed for the BB-I···Ar cluster cation are summarized in Table 3. The strong similarity of the intramolecular modes compared to the monomer confirms that the assignment of the REMPI peak at 37522 cm^{-1} to BB-I···Ar is correct and UMP2 calculation gives the reasonable agreement of our experimental results.

4.3. MATI Spectrum of *n*-Butylbenzene-V···Ar. Figure 4 displays the MATI spectrum of the *anti*-conformers of BB-V···Ar obtained *via* the $S_1 0^0$ vibrationless origin. The prominent feature at 69845 ± 5 cm^{-1} is again assigned as the IE because no additional spectral features were observed in the lower energy spectral range.

We tentatively assign the peak appearing at 47 cm^{-1} to the torsion mode, τ_a'', which is predicted at 53 cm^{-1} in calculated UMP2 harmonic vibrational frequencies. However, we cannot rule out that the intermolecular stretch mode s_Z, which is predicted at 52 cm^{-1}, may overlap with τ_a'' due to the lack of resolution in this MATI spectrum. The scissor bending mode B_{c7}' and its three quanta progression appear at 66 and 198 cm^{-1}, respectively. The bending mode, β', and the stretch mode, σ', are also observed at 173 and 248 cm^{-1}, respectively. The similarity of those intramolecular modes observed in the monomer[14] and Ar cluster of BB-V once more confirms the assignment of the BB-V···Ar in the REMPI spectrum. The absence of the intermolecular vibrational modes b_X and b_Y probably indicates that there is a modest ionization-induced geometry charge of the Ar atom position in the b_X and b_Y coordinates on the plane of the aromatic ring. Table 4 lists all the observed features of the BB-V···Ar cluster cation observed compared with the vibrational modes observed in BB-V monomer. Our UMP2 calculation results are in line with those features and the intramolecular vibrational modes have changed very little compared to the BB-V monomer calculation.[14]

5. Further Discussion

Table 5 summarizes the calculated results of stabilization energy and experimental results of excitation and ionization energies of the BB···Ar clusters. For comparing the difference between BB-I···Ar and BB-V···Ar energy levels, the energetics diagram is shown in Figure 5. With the CCSD(T)/CBS level of theory giving stabilization energies of 650 and 558 cm^{-1} for BB-I···Ar and BB-V···Ar, respectively, the stabilization energy of the neutral excited S_1 state decreases to 641 cm^{-1} for BB-I···Ar and increases to 578 cm^{-1} for BB-V···Ar. Due to the ion-induced dipole interaction for the cation clusters, both clusters have significantly increased stabilization energies of 746 and 668 cm^{-1} for BB-I···Ar and BB-V···Ar, respectively. Compared with S_0 and D_0 states of benzene···Ar, with stabilization energies of 340 and 575 cm^{-1}, respectively,[40,41] the BB-I···Ar and BB-V···Ar cluster seems more stable. This is probably because the extra interactions between the alkyl side chains and the Ar atom can further stabilize the cluster.

ZEKE and MATI spectra for the series of alkylbenzene···Ar clusters including BB···Ar in this paper have been recorded over the low-energy region of the cationic ground state. Table 6 lists their IE shifts along with the IEs of the monomer and argon clusters. All the alkylbenzene clusters display red shifts of the IEs upon Ar complexation. This is due to changes in the intermolecular interaction upon ionization. The vdW bonding strength between the monomer and argon atom is greatly enhanced by the ion-induced dipole interaction that is present in the cationic clusters compared to the dipole-induced interaction of the neutral ground state. The red shift is reduced along with the increase of the alkyl side chain. This is because the conjugation effect increases and the charge on the aromatic ring is more efficiently transferred to the alkyl side chain for the longer alkyl side chains in the cationic states.

Furthermore, it is interesting to compare the red shifts for the BB-I···Ar and BB-V···Ar complexes. The smaller red shift observed for the *gauche*-conformer cluster BB-I^+···Ar indicates

TABLE 6: Adiabatic Ionization Energies (in cm^{-1}) and Respective Complexation Shifts (in cm^{-1}) of the Alkylbenzenes and Their Argon Clusters Obtained Using ZEKE/MATI Spectroscopy

molecule			IE(monomer)	IE(argon cluster)	IE shift
benzene[42,43]		−H	74555	74383	−172
toluene[44]		$-CH_3$	71203	71037	−166
ehylbenzene[45]		$-CH_2CH_3$	70762	70634	−128
n-propylbenzene[46]		$-(CH_2)_2CH_3$	70272	70160	−112
n-butyl-benzene	(I)	$-(CH_2)_3CH_3$	70148	70052	−96
n-butyl-benzene	(V)	$-(CH_2)_3CH_3$	69955	69845	−110

a relatively weaker binding of the Ar atom compared to the *anti*-conformer cluster, BB-V^+···Ar. This may reflect that the repulsive interaction between some hydrogen atoms in the alkyl side chain and ion-induced positive side of Ar atom in the *gauche*-conformers I increases its ionization energy. The other possible explanation is that the alkyl side chain in conformer I of BB, which is bent back close to the aromatic ring, can have stronger conjugation effects than the fully extended alkyl side chain in conformer V of BB. Therefore, stronger charge transfer to the alkyl side chain can weaken the ion-induced dipole interaction between Ar and the aromatic ring.

Supporting Information Available: Tables of *xyz* coordinates. This material is available free of charge *via* the Internet at http://pubs.acs.org.

References and Notes

(1) Glusker, J. P. Directional aspects of intermolecular interactions. In *Design of Organic Solids*; Springer: New York, 1998; Vol. 198; pp 1.

(2) Nangia, A.; Desiraju, G. R. Supramolecular synthons and pattern recognition. In *Design of Organic Solids*, Springer: New York, 1998; Vol. 198; pp 57.

(3) Shilov, I. Y.; Kurnikova, M. G. *J. Phys. Chem. B* **2003**, *107*, 7189.

(4) Forde, G. K.; Kedzierski, P.; Sokalski, W. A.; Forde, A. E.; Hill, G. A.; Leszczynski, J. *J. Phys. Chem. A* **2006**, *110*, 2308.

(5) Dziekonski, P.; Sokalski, W. A.; Podolyan, Y.; Leszczynski, J. *Chem. Phys. Lett.* **2003**, *367*, 367.

(6) Moarefi, I.; LaFevreBernt, M.; Sicheri, F.; Huse, M.; Lee, C. H.; Kuriyan, J.; Miller, W. T. *Nature* **1997**, *385*, 650.

(7) Benhorin, N.; Even, U.; Jortner, J. *J. Chem. Phys.* **1989**, *91*, 331.

(8) Neusser, H. J.; Krause, H. *Chem. Rev* **1994**, *94*, 1829.

(9) Zhang, X.; Knee, J. L. *Faraday Discuss* **1994**, *97*, 299.

(10) Pitts, J. D.; Knee, J. L. *J. Chem. Phys.* **1998**, *109*, 7113.

(11) Lembach, G.; Brutschy, B. *J. Phys. Chem.* **1996**, *100*, 19758.

(12) Grebner, T. L.; Unold, P. V.; Neusser, H. J. *J. Phys. Chem. A* **1997**, *101*, 158.

(13) Dessent, C. E. H.; Müller-Dethlefs, K. *Chem. Rev.* **2000**, *100*, 3999.

(14) Tong, X.; Ford, M. S.; Dessent, C. E. H.; Müller-Dethlefs, K. *J. Chem. Phys.* **2003**, *119*, 12908.

(15) Ford, M. S.; Tong, X.; Dessent, C. E. H.; Müller-Dethlefs, K. *J. Chem. Phys.* **2003**, *119*, 12914.

(16) Tong, X.; Černý, J.; Müller-Dethlefs, K.; Dessent, C. E. H. *J. Phys. Chem. A* **2008**, *112*, 5866.

(17) Suzuki, K.; Ishiuchi, S.; Sakai, M.; Fujii, M. *J J. Electron Spectrosc. Relat. Phenom.* **2005**, *142*, 215.

(18) Georgiev, S.; Neusser, H. J. *J. Electron Spectrosc. Relat. Phenom.* **2005**, *142*, 207.

(19) Choi, K. J.; Kim, S. K.; Ahn, D. S.; Lee, S. *J. Phys. Chem.* **2004**, *108*, 11292.

(20) Müller-Dethlefs, K.; Dopfer, O.; Wright, T. G. *Chem. Rev* **1994**, *94*, 1845.

(21) Kimura, K. *J. Electron Spectrosc. Relat. Phenom.* **2000**, *108*, 31.

(22) Atkins, P. W. *Physical Chemistry*5th ed.; Oxford University Press: Oxford, U.K., 1994.

(23) Janzen, A. R.; Aziz, R. A. *J. Chem. Phys.* **1997**, *107*, 914.

(24) Aziz, R. A.; Janzen, A. R.; Moldover, M. R. *Phys. Rev. Lett.* **1995**, *74*, 1586.

(25) Burda, J. V.; Zahradnik, R.; Hobza, P.; Urban, M. *Mol. Phys.* **1996**, *89*, 425.

(26) van Mourik, T.; Dunning, T. H. *J. Chem. Phys.* **1999**, *111*, 9248.

(27) Ford, M. S.; Haines, S. R.; Pugliesi, I.; Dessent, C. E. H.; Müller-Dethlefs, K. *J. Electron Spectrosc. Relat. Phenom.* **2000**, *112*, 231.

(28) Haines, S. R.; Geppert, W. D.; Chapman, D. M.; Watkins, M. J.; Dessent, C. E. H.; Cockett, M. C. R.; Müller-Dethlefs, K. *J. Chem. Phys.* **1998**, *109*, 9244.

(29) Dessent, C. E. H.; Haines, S. R.; Müller-Dethlefs, K. *Chem. Phys. Lett.* **1999**, *315*, 103.

(30) Gerstenkorn, S.; Luc, P. *Atlas Du Spectre D'absorption De La Molecule D'iode*; CNRS: Orsay, France, 1978.

(31) Chupka, W. A. *J. Chem. Phys.* **1993**, *98*, 4520.

(32) Frisch, M. J.; Trucks, G. W.; Schlegel, H. B.; Scuseria, G. E.; Robb, M. A.; Cheeseman, J. R.; Montgomery, J. A., Jr.; Kudin, K. N.; Burant, J. C.; Millam, J. M.; Iyengar, S. S.; Tomasi, J.; Barone V.; Mennucci, B.; Cossi, M.; Scalmani, G.; Rega, N.; Petersson, G. A.; Nakatsuji, H.; Hada, M.; Ehara, M.; Toyota, K.; Fukuda, R.; Hasegawa, J.; Ishida, M.; Nakajima, T.; Honda, Y.; Kitao, O.; Nakai, H.; Klene, M.; Li, X.; Knox, J. E.; Hratchian, H. P.; Cross, J. B.; Adamo, C.; Jaramillo, J.; Gomperts, R.; Stratmann, R. E.; Yazyev, O.; Austin, A. J.; Cammi, R.; Pomelli, C.; Ochterski, J. W.; Ayala, P. Y.; Morokuma, K.; Voth, G. A.; Salvador, P.; Dannenberg, J. J.; Zakrzewski, V. G.; Dapprich, S.; Daniels, A. D.; Strain, M. C.; Farkas, O.; Malick, D. K.; Rabuck, A. D.; Raghavachari, K.; Foresman, J. B.; Ortiz, J. V.; Cui, Q.; Baboul, A. G.; Clifford, S.; Cioslowski, J.; Stefanov, B. B.; Liu, G.; Liashenko, A.; Piskorz, P.; Komaromi, I.; Martin, R. L.; Fox, D. J.; Keith, T.; Al-Laham, M. A.; Peng, C. Y.; Nanayakkara, A.; Challacombe, M.; Gill, P. M. W.; Johnson, B.; Chen, W.; Wong, M. W.; Gonzalez, C.; Pople, J. A. *Gaussian 03*, version C.02; Gaussian, Inc.: Wallingford, CT, 2004.

(33) Černý, J.; Tong, X. ; Hobza, P.; Müller-Dethlefs, K. J. Chem. Phys., in press.

(34) Halkier, A.; Helgaker, T.; Jorgensen, P.; Klopper, W.; Koch, H.; Olsen, J.; Wilson, A. K. *Chem. Phys. Lett.* **1998**, *286*, 243.

(35) Jurecka, P.; Hobza, P. *Chem. Phys. Lett.* **2002**, *365*, 89.

(36) Jurecka, P.; Hobza, P. *J. Am. Chem. Soc.* **2003**, *125*, 15608.

(37) Werner, H.-J.; Knowles, P. J. with contributions from Almlof, J.; Amos, R. D.; Berning, A.; Celani, P.; Cooper, D. L.; Deegan, M. J. O.; Dobbyn, A. J.; Eckert, F.; Elbert, S. T.; Hampel, C.; Hetzer, G.; Lindh, R.; Lloyd, A. W.; Meyer, W.; Nicklass, A.; Korona, T.; Peterson, K.;. Pitzer, R.; Rauhut, G.; Stone, A. J.; Taylor, P. R.; Mura, M. E.; Pulay, P.; Schutz, M.; Stoll, H.; Thorsteinsson, T. *MOLPRO, a package of ab initio programs*.

(38) Černý, J.; Tong, X.; Hobza, P.; Müller-Dethlefs, K. *Phys. Chem. Chem. Phys.*, submitted for publication.

(39) Chervenkov, S.; Karaminkov, R.; Braun, J. E.; Neusser, H. J.; Panja, S. S.; Chakraborty, T. *J. Chem. Phys.* **2006**, *124*, 234302.

(40) Krause, H.; Neusser, H. J. *J. Chem. Phys.* **1993**, *99*, 6278.

(41) Hobza, P.; Bludsky, O.; Selzle, H. L.; Schlag, E. W. *J. Chem. Phys.* **1992**, *97*, 335.

(42) Chewter, L. A.; Sander, M.; Müller-Dethlefs, K.; Schlag, E. W. *J. Chem. Phys.* **1987**, *86*, 4737.

(43) Chewter, L. A.; Müller-Dethlefs, K.; Schlag, E. W. *Chem. Phys. Lett.* **1987**, *135*, 219.

(44) Lu, K. T.; Eiden, G. C.; Weisshaar, J. C. *J. Phys. Chem.* **1992**, *96*, 9742.

(45) Sato, S.; Byodo, K.; Kojima, T.; Shinohara, H.; Yanagihara, S.; Kimura, K. *J. Electron Spectrosc. Relat. Phenom.* **2000**, *112*, 247.

(46) Takahashi, M.; Kimura, K. *J. Chem. Phys.* **1992**, *97*, 2920.

JP710998M